

Er³⁺ photoluminescence properties of erbium-doped Si/SiO₂ superlattices with subnanometer thin Si layers

Yong Ho Ha and Sehun Kim

Department of Chemistry, School of Molecular Science, Korea Advanced Institute of Science and Technology (KAIST), 373-1 Kusung-dong, Yusung-Gu, Taejeon, Korea

Dae Won Moon

Nano Surface Group, Korea Research Institute of Standards and Science (KRISS), Doryong-dong 1, Taejeon 305-606, Korea

Ji-Hong Jhe and Jung H. Shin

Department of Physics, Korea Advanced Institute of Science and Technology (KAIST), 373-1 Kusung-dong, Yusung-gu, Taejeon, Korea

(Received 1 February 2001; accepted for publication 15 May 2001)

The effect of the Si layer thickness on the Er³⁺ photoluminescence properties of the Er-doped Si/SiO₂ superlattice is investigated. We find that the Er³⁺ luminescence intensity increases by over an order of magnitude as the Si layer thickness is reduced from 3.6 nm down to a monolayer of Si. Temperature dependence of the Er³⁺ luminescence intensity and time-resolved measurement of Er³⁺ luminescence intensity identify the increase in the excitation rate as the likely cause for such an increase, and underscore the importance of the Si/SiO₂ interface in determining the Er³⁺ luminescence properties. © 2001 American Institute of Physics. [DOI: 10.1063/1.1383802]

Since the work by Ennen *et al.*,¹ the Er doping of silicon has received a great deal of attention as it promises the possibility of developing Si-based optoelectronics. In particular, Si nanostructures such as Si nanoclusters^{2–4} and Si/SiO₂ superlattices⁵ are being recognized as an attractive alternative to bulk Si for Er doping as they show much less temperature- and carrier-induced quenching of Er³⁺ luminescence than bulk Si.^{6,7}

An additional advantage of using the Si/SiO₂ superlattice for Er doping is that the location and environment of Er can be controlled precisely. Recently, we have demonstrated using buffer layers of pure SiO₂ that such a precise control can result in an increase of Er³⁺ luminescence intensity by several orders of magnitude and a near complete suppression of the temperature quenching of Er³⁺ luminescence.⁵ In this letter, we investigate the effects of varying the Si layer thickness on the Er³⁺ photoluminescence (PL) properties of Er-doped Si/SiO₂ superlattices. We find that as the Si layer thickness is reduced from 3.6 nm down to a monolayer, Er³⁺ PL intensity increases by over an order of magnitude. The temperature dependence and the time-resolved measurements of the Er³⁺ PL intensity suggest the increase in the excitation rate as the likely cause for such an increase. The results underscore the importance of the Si/SiO₂ interface in determining the Er³⁺ luminescence, and suggest that for high efficiency, the surface/volume ratio of Si regions should be increased.

Er-doped Si/SiO₂ superlattices were deposited by UHV sputter deposition of Si using 500 eV Ar⁺ beam. Er-doped SiO₂ layers were deposited by co-sputtering Si and Er in an oxygen atmosphere. Only the SiO₂ layers were doped with Er. The growth rate of both Si- and the Er-doped SiO₂ layers was ~0.014 nm/s. The SiO₂ layer thickness was fixed at 9.6 nm, but the nominal Si layer thickness was varied from 0.6 to 3.6 nm. The Er concentration in the SiO₂ layers was 0.5

at. %. The total number of periods was fixed at 20 for all samples, and a 5-nm-thick cap layer of Si was deposited to protect the film. After deposition, the films were rapid thermal annealed in a flowing Ar environment. An anneal sequence of 20 min at 600 °C, 5 min at 950 °C, and 5 min at 600 °C was used to avoid cracking and spalling of the films. Deposited films were analyzed using transmission electron microscopy (TEM) and medium energy ion scattering spectroscopy (MEIS). MEIS spectra were taken using 101 keV H⁺ beam aligned to the [001] direction in the (001) plane, and the scattering angle of 106.3°. The Er³⁺ PL spectra were measured using an Ar laser, a grating monochromator, a thermoelectrically cooled InGaAs detector, and the standard lock-in technique. The nominal laser power was 200 mW. The 477 nm line of Ar laser was used to ensure that Er³⁺ ions are excited only via carriers and not through direct optical absorption. Low temperature PL spectra were measured using a closed-cycle helium cryostat, and time-resolved PL intensities were measured using a digitizing oscilloscope.

Figure 1 shows the TEM images of the deposited and annealed films with nominal Si layer thicknesses of 1.8 and 2.4 nm. Good planarity and agreement with expected layer thicknesses are observed. We note that the Si layers are amorphous despite the high temperature anneal. This is in agreement with results of other researchers,⁸ and is attributed to the thinness of the Si layers.

To analyze the films with thinner Si layers, MEIS was used because no conclusive determination of the Si layer thickness could be made with TEM. The result for the film with the nominal Si layer thickness of 0.8 nm is shown in Fig. 2. The symbols are experimental data, and the line is the simulated fit to the data. In fitting the data, we have allowed for the possibility of nonelemental Si layers by performing a multidimensional fit with varying Si and O content. As shown in the inset, we obtain the best result if we assume a

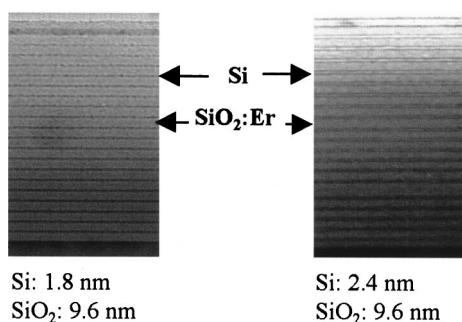


FIG. 1. Bright-field cross-section TEM images of the superlattice films with Si layer thicknesses of 1.8 and 2.4 nm. The thin, dark bands are Si layers, and the thick, gray bands are the SiO₂ layers. No crystalline grains or diffraction patterns could be observed, indicating that the layers are amorphous.

pure Si layer that is 1.3 monolayer thick, which indicates that we still have an ultrathin, continuous Si layer. Similar fit to the film with the nominal Si layer thickness of 0.6 nm indicated the presence of a continuous Si layer of 1 monolayer thickness (not shown).

All films displayed the typical Er³⁺ luminescence near 1.54 μ m due to the $^4I_{13/2} \rightarrow ^4I_{15/2}$ intra- $4f$ transition of Er³⁺ (not shown). The temperature dependence of the integrated Er³⁺ PL intensities is shown in Fig. 3. We find that as the Si layer thickness decreases, the Er³⁺ luminescence intensity *increases* monotonically by over an order of magnitude. At its highest value, the Er³⁺ PL intensity is quite intense, and is similar to that of Er-doped Si/SiO₂ superlattices with buffer layers of pure SiO₂.⁵ The temperature dependence of the Er³⁺ PL intensity, on the other hand, is nearly the same for all films. In all cases, the Er³⁺ PL intensity decreases by $\sim 50\%$ as the temperature is raised from 25 K to room temperature.

In order to confirm that the effects observed in Fig. 3 are not optical artifacts, we have calculated the near-normal reflectivity of the superlattice films using the transfer matrix method (not shown). The calculated reflectivities were all within 50%–70% range. Furthermore, varying the pump laser wavelength from 457 to 515 nm did not result in any significant differences in the relative Er³⁺ PL intensities,

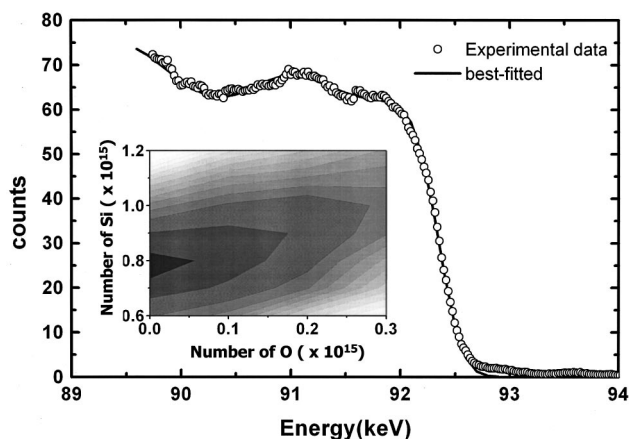


FIG. 2. The MEIS spectra of the film with nominal Si layer thickness of 0.8 nm. The symbols are the experimental data, and the line is the result of the fit. The inset shows the result of the multidimensional fit. Dark regions indicate a better fit to the data.

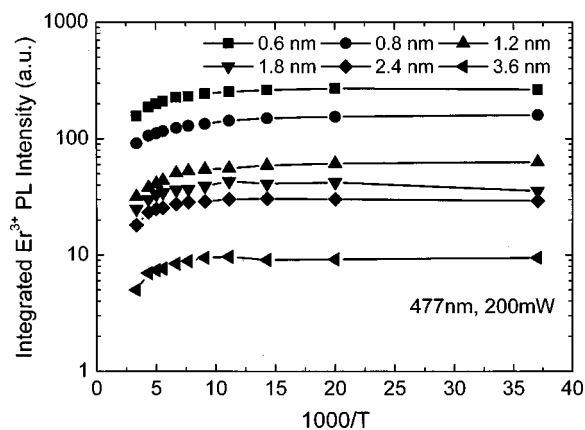


FIG. 3. The temperature dependence of the integrated 1.54 μ m Er³⁺ PL intensities of the superlattice films.

confirming that the increase observed in Fig. 3 is real and not an optical artifact.

It should also be noted that without the Si layers, virtually no Er³⁺ PL can be observed since the 477 nm excitation light is not absorbed optically by Er³⁺ ions. For comparison, a pure SiO₂ film without Si layers doped with Er was deposited, and excited optically using the 488 nm line of the Ar laser under identical conditions. Its room temperature Er³⁺ PL intensity was about eight times less intense than that of the superlattice film with thinnest Si layers, demonstrating the advantage of using the superlattice structure.

Since the total number and the environment of Er are same in all samples, the increase in the Er³⁺ PL intensity observed in Fig. 3 indicates that the excitation rate of Er³⁺ increases, and/or that the nonradiative decay rate of excited Er³⁺ decreases as the Si layer thickness is reduced. It is by now well established that the dominant nonradiative decay mechanisms of Er³⁺ in Si are Auger-type interactions with carriers, and that they are responsible for the temperature quenching of Er³⁺ luminescence.^{6,7} However, as shown in Fig. 3, the temperature quenching of Er³⁺ luminescence is nearly the same for all films, suggesting that the carrier-mediated de-excitation rate does not depend strongly on the Si layer thickness. The Er³⁺ excitation rate, on the other hand, *increases* as the Si layer thickness decreases. This is shown in Fig. 4, which shows the time-resolved Er³⁺ luminescence intensity. Only the films with a Si layer thickness of

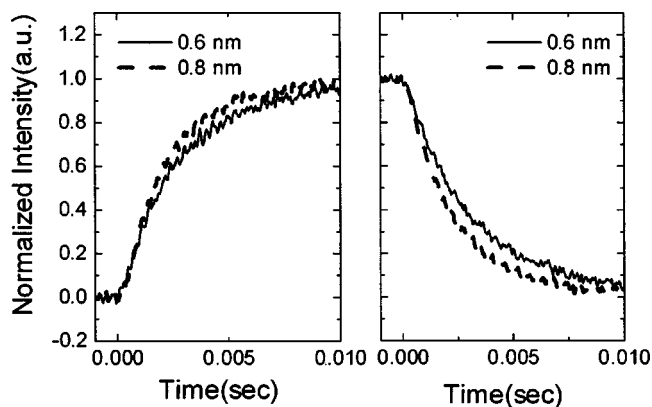


FIG. 4. The rise and decay trace of the Er³⁺ luminescence of the films with Si layer thickness of 0.8 and 0.6 nm. The excitation rate, defined as $1/\tau_{\text{rise}} - 1/\tau_{\text{decay}}$ for the two films are 10 and 30 s⁻¹, respectively.

0.8 and 0.6 nm are analyzed because only they gave enough signal to accurately determine the luminescence decay traces. If we model the excitation of Er as a simple two-level system, then the excitation rate, W_{exc} , is simply given by $1/\tau_{\text{rise}} = W_{\text{exc}} + 1/\tau_{\text{decay}}$. Determining τ by integrating the traces, we find that the excitation rate of Er^{3+} increases from 10 to 30 s^{-1} as the Si layer thickness is decreased from 0.8 to 0.6 nm.

The temperature quenching of Er^{3+} luminescence has been correlated with the bandgap of the host material.⁹ Therefore, the fact that all films show a similar temperature dependence of the Er^{3+} luminescence indicates that in this case, the quantum confinement effects do not play a major role in determining the Er^{3+} luminescence. This is attributed to the fact that the Si layers are amorphous. First, the carrier localization radius in *a*-Si is less than 1 nm,¹⁰ making quantum confinement difficult. Second, since the band gap of bulk *a*-Si is already wide enough to substantially suppress temperature quenching of Er^{3+} luminescence by itself, the effects of any further increase will be small.

The amorphous nature of Si layers can also help understand how the Er^{3+} excitation rate can increase with thinner Si layers even though we have less absorption of the pump beam. Because of the high anneal temperature, very little hydrogen is expected to be left in the film. Such pure *a*-Si, however, can contain as many as 10^{20} cm^{-3} defects¹¹ with carrier capture cross sections that are much larger than the carrier-mediated excitation cross section of Er^{3+} in Si.¹² Indeed, pure *a*-Si doped with Er is known to show near complete suppression of Er^{3+} luminescence.¹³ Therefore, only carriers generated near the Si/SiO₂ interfaces are likely to contribute significantly to excitation of Er doped into the SiO₂ layers. The bulk region of the Si layers will not only contribute minimally to excitation of Er^{3+} , but will in fact compete strongly with Er^{3+} ions for carriers generated by the incident light. Reducing the volume of the bulk region from the *a*-Si layers will reduce such competing trap densities, and thus increase the Er^{3+} excitation rate, as is observed. Note that because some Si-rich region is necessary for carrier generation, there will be an optimum interface/volume ratio. The fact that a single monolayer of Si is sufficient, however, shows that the ratio is very large. It is also possible that the defects in *a*-Si layers act as nonradiative decay paths for excited Er^{3+} ions. Conclusive evidence of this effect, however, is difficult to obtain since films with thicker Si layers have higher refractive indices, and thus higher radiative decay rates of Er^{3+} .¹⁴

The above conclusion has several implications. First, many results suggest that the Er^{3+} luminescence from Er-doped Si nanostructures is dominated from Er^{3+} ions located inside the SiO₂ matrix near the Si/SiO₂ interface.^{4,5,14} Thus, above results suggest that the large surface/volume ratios that occur naturally in nanostructures may be a part of the reason behind the high Er^{3+} luminescence efficiencies reported

from Er-doped Si nanostructures. Then in order to obtain the highest Er^{3+} luminescence, the interface/volume ratio should be increased as much as possible—e.g., it would be better to form a large number of very small nanoclusters or very thin Si layers than to form a small number of larger clusters or thicker Si layers. Second, a promising application of Er-doped Si nanostructures is waveguide amplifiers for the 1.54 μm light. Not only is the Er^{3+} excitation efficiency very high, but the pump laser can be eliminated as well, since the incident light only has to generate carriers. However, the presence of free carriers can lead to the nonradiative decay of Er^{3+} ions and free-carrier absorption of the 1.54 μm light that severely degrade the performance of such amplifiers.¹⁴ The results presented here show that by using ultrathin Si layers to eliminate the bulk region, it may be possible to significantly reduce the presence of free carriers while still retaining the efficiency of carrier-mediated excitation.

In conclusion, we have demonstrated fabrication of Er-doped Si/SiO₂ superlattices with subnanometer control of the Si layer thickness. The Er^{3+} luminescence increased with decreasing Si layer thickness all the way down to a monolayer of Si. Based on the temperature dependence and time-resolved measurement of Er^{3+} luminescence, we identify the reduction of the bulk-Si region as the main reason for such an increase. Based on these results, we suggest that for device applications, a large number of ultrathin Si layers or high density of very small Si nanoclusters are preferable.

This work was supported in part by Advanced Photonics Project, the University Research Program supported by Ministry of Information and Communications in South Korea, the National Research Laboratory Program by the MOST of Korea, and the Brain Korea 21 Project.

¹H. Ennen, J. Schneider, G. Pomrenke, and A. Axmann, Appl. Phys. Lett. **43**, 943 (1983).

²A. J. Kenyon, P. F. Trwoga, M. Federighi, and C. W. Pitt, J. Phys.: Condens. Matter **6**, L319 (1994).

³M. Fujii, M. Yoshida, Y. Kanazawa, S. Hayashi, and K. Yamamoto, Appl. Phys. Lett. **71**, 1198 (1997).

⁴J. H. Shin, S.-Y. Seo, S. Kim, and S. G. Bishop, Appl. Phys. Lett. **76**, 1999 (2000).

⁵J. H. Shin, J.-H. Jhe, S.-Y. Seo, Y. H. Ha, and D. W. Moon, Appl. Phys. Lett. **76**, 3567 (2000).

⁶J. Palm, F. Gan, B. Zheng, J. Michel, and L. C. Kimerling, Phys. Rev. B **54**, 17603 (1996).

⁷F. Priolo, G. Franzó, S. Coffa, and A. Carnera, Phys. Rev. B **57**, 4443 (1998).

⁸M. Zacharias, J. Blasing, P. Veit, L. Tsybeskov, K. Hirschman, and P. M. Fauchet, Appl. Phys. Lett. **74**, 2614 (1999).

⁹P. N. Favenec, H. L'Haridon, D. Moutonnet, M. Salvi, and M. Ganneau, Mater. Res. Soc. Symp. Proc. **301**, 181 (1993).

¹⁰Y. Kanemitsu, Y. Fukunishi, and T. Kushida, Appl. Phys. Lett. **77**, 211 (2000).

¹¹P. Stolk, Ph. D. thesis, Utrecht University, the Netherlands, 1993.

¹²A. Polman, G. N. van den Hoven, J. S. Custer, J. H. Shin, R. Serna, and P. F. A. Alkemade, J. Appl. Phys. **77**, 1256 (1995).

¹³J. S. Custer, E. Snoeks, and A. Polman, Mater. Res. Soc. Symp. Proc. **235**, 51 (1992).

¹⁴P. G. Kik and A. Polman, J. Appl. Phys. **88**, 1992 (2000).